Journal Pre-proofs

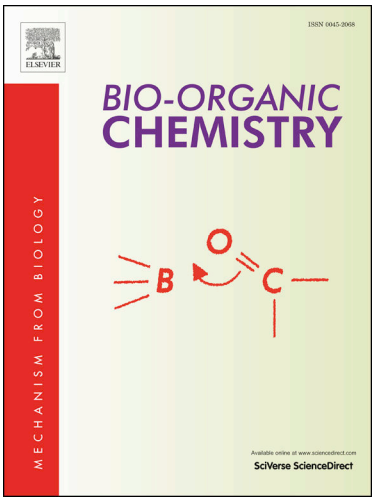

Synthesis, Crystal Structure and Hirshfeld Analysis of Benzamide Derivatives of Thiourea as Potent Inhibitors of α-Glucosidase in-vitro

Sidra Akhter, Saeed Ullah, SammerYousuf, Atia-tul-Wahab, Hina Siddiqui, M. Iqbal Choudhary

PII: S0045-2068(20)31829-0
DOI: https://doi.org/10.1016/j.bioorg.2020.104531
Reference: YBIOO 104531

To appear in: *Bioorganic Chemistry*

Received Date: 4 April 2020
Revised Date: 1 December 2020
Accepted Date: 2 December 2020

Please cite this article as: S. Akhter, S. Ullah, SammerYousuf, Atia-tul-Wahab, H. Siddiqui, M. Iqbal Choudhary, Synthesis, Crystal Structure and Hirshfeld Analysis of Benzamide Derivatives of Thiourea as Potent Inhibitors of α-Glucosidase in-vitro, *Bioorganic Chemistry* (2020), doi: https://doi.org/10.1016/j.bioorg.2020.104531

Synthesis, Crystal Structure and Hirshfeld Analysis of Benzamide Derivatives of Thiourea as Potent Inhibitors of α-Glucosidase in-vitro

Sidra Akhter[a], Saeed Ullah[a], SammerYousuf[a], Atia-tul-Wahab[b], Hina Siddiqui*[a], and M. Iqbal Choudhary*[a,b,c]

[a]H.E.J. Research Institute of Chemistry, International Center for Chemical and Biological Sciences, University of Karachi, Karachi-75270, Pakistan

[b]Dr. Panjwani Center for Molecular Medicine and Drug Research, International Center for Chemical and Biological Sciences, University of Karachi, Karachi-75270, Pakistan

[c]Department of Biochemistry, Faculty of Science, King Abdulaziz University, Jeddah-21452, Saudi Arabia

ABSTRACT

Benzamide based structural analogues **1-15** were synthesized, and evaluated for α-glucosidase inhibition activity *in vitro* for the first time. Compounds **1-9** were found to be known, while compounds **10-15** were found to be new. However, to the best of our knowledge we are reporting α-glucosidase inhibitory activity of these bezamide derivatives of thiourea for the first time. Compounds **1**, **3**, **6-8**, **10-14** were found to be potent inhibitors of α-glucosidase within IC_{50} range of 20.44-333.41 µM, in comparison to the standard inhibitor, acarbose (IC_{50}=875.75±2.08 µM). Mode of the enzyme inhibition was determined on the basis of kinetic studies which demonstrated that compounds **8**, and **10** were non-competitive and competitive inhibitors of α-glucosidase enzyme, respectively. These compoundswere also evaluated for their DPPH radical scavenging activity, and cytotoxicity against 3T3 mouse fibroblast cell lines. All synthesized compounds showed a significant to moderate DPPH radical scavenging activity and appeared to be non-cytotoxic except compound **9** which showed cytotoxicity against 3T3 normal mouse fibroblast cell lines. A single crystal X-ray and Hirshfeld Surface analysis of a representative compound is also presented.

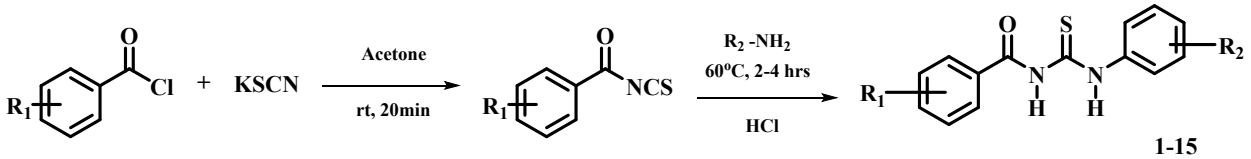

1-15

Key words: 1-Benzamide derivatives, 2- Thiourea derivatives, 3- α-Glucosidaseinhibitors, 4- Diabetes, 5- Hirshfeld analysis

1.0: INTRODUCTION

α-glucosidase (EC 3.2.1.20) is an exo-type glycosidase enzyme, present on the brush boarders of small intestine, and catalyzes the hydrolysis of carbohydrates from non-reducing end, yielding glucose molecules. α-Glucosidase inhibitors (AGIs) slowdown the absorption of glucose into blood, thus control the postprandial hyperglycemia.AGIs also provide cardiovascular benefits [1]. AGI's have been termed as 'untapped diamonds' of diabeteology and also referred as starch blocker [2].Therefore, α-glucosidase inhibition has become an important strategy for the management of type 2 diabetes. Unlike most other types of diabetic drugs, they do not have a direct effect on insulin secretion instead they work by slowing down the digestion of carbohydrates. Although AGI's are effective therapies against diabetes, they are also known to be associated with various adverse effects, including abdominal bloating caused by fermentation of unabsorbed carbohydrate, diarrhea, cramping, and colonic gas production [3]. Therefore, there is a need of new, safe, and effective inhibitors of α-glucosidase enzyme for the treatment of type 2 diabetes mellitus.

Thiourea forms an important class of organic compounds with diverse applications in the field of coordination chemistry, therapeutic, metallurgy, analytical and agriculture chemistry [4-7]. Benzamide derivatives of thiourea are known to have a wide range of medicinal properties [8], including anti-provocative [9], anti-obesity [10, 11], anti-bacterial [12, 13], anti-fungal [14, 15] anti-glycation [16, 17], and carbonic anhydrase inhibition [18] activities. Metal complexes of derivatives of thiourea are also well known for their biological activities [19-21] and also reported to be used for cationic separation of metals [22, 23].

During the current study, phenyl substituted derivatives of thiourea (**1-15)** were synthesized. All synthesized derivatives were found to be new except compounds **1-9**. An *in-vitro* mechanism-based biochemical screening has also been performed to evaluate their α-glucosidase inhibitory activity. To the best of our knowledge, all the derivatives studied in this study are reported for the first time as inhibitors of α-glucosidase enzyme. Compounds **1**, **3**, **6-8**, **13**, and **10-14** were found to be potent inhibitors ofα-glucosidase enzyme as compared to the standard Acarbose (IC_{50}=875.75±2.08 μM). All synthesized derivatives **1-15** were also evaluated for their cytotoxic effect on 3T3 normal fibroblast cell lines and DPPH radical scavenging activity. A single crystal X-ray and Hirshfeld Surface analysis of a representative compound is also presented.

2.0: Experimental

2.1. General experimental conditions

The ^{1}H-NMR spectra were acquired on Avance 300, 400, 500 and 600 MHz spectrometers (Bruker Switzerland) using DMSO-d_6. EI-MS analysis was carried out on JEOL JMS-600 mass spectrometer with associated data system of MASPEC. Melting points of compounds were recorded on Buchi 434 an electro-thermal melting point equipment. TLC analyses were carried on pre-coated ALUGRAM, SIL, G/UV254 aluminum plates (Kieselgel 60, 20 x 20, 0.5mm thick, E, Merck, Germany). Ultraviolet light of 254 nm was used to observe fluorescence quenching spots, and 365 nm was used for visualization of thin layer chromatogram.

2.2. General synthetic procedure

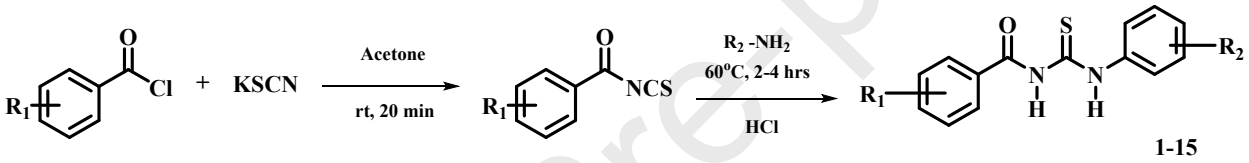

Scheme 1: General reaction scheme for the synthesis of benzamide derivatives of thiourea **1-15**.

Compounds **1-15** were synthesized by the procedure described by Binzet and co-workers [24]. Substituted benzoyl chloride (1 mmol) was dissolved, followed by addition of 10 mL, *i.e*. 1 mmol solution of potassium thiocynate in dry acetone and allowed to reflux for 20 minutes. After 20 minutes, mixture was cooled to room temperature, and 6 mL solution of 1 mmol primary amine, prepared in dry acetone, was added into it with continuous stirring. After 2 hours, 5 mL of 0.2 N HCl was added to obtained solid product which was washed with hexane and ethylacetate (9:1) and recrystallized from 2:1 mixture of dichloromethane: methanol.

All the derivatives were obtained in amorphous state, except compounds **5**, and **6**, which were obtained in crystalline state. In EI-MS all synthesized thiourea derivatives showed the molecular ion peak (M^+) except compound **3,** that yielded molecular ion peak *via*soft technique ESI-MS. FT-IR spectra were taken within the range of 4000-400 $cm^{-1}$by using KBr pellets. The ^{1}H-NMR data for all compounds was recorded in DMSO-d_6 at 400 MHz.^{13}C-NMR experiments were conducted

in DMSO-d_6 for compounds **13**, and **14** at100MHz instrument. UV absorptionstudies were carried out between 250 to 400 nm.

2.2.1. *N*-(Phenylcarbamothioyl)benzamide (1):

White. Yield: 72%, m. p. 144-152 °C. FT-IR (KBr pellet cm^{-1}): ν_{max} (N-H) 3285; (C-H) 2925; (C=S) 1261.λ_{max}, nm (CH_3OH) (ϵ, $M^{-1}cm^{-1}$): 212 (7271); 261 (10928);^{1}H-NMR (400 MHz, DMSO-d_6): δ 12.59 (1H, s, N-H), 11.54 (1H, s, N-H), 7.97 (2H, d, $J_{2',6'}$ = 7.5Hz, H-2′, H-6′), 7.53 (2H, t, $J_{3'(2',4')}$ =$J_{5'(4',6')}$= 7.7 Hz, H-3′,H-5′). 7.26 (1H, t, $J_{4'(3',5')}$= 7.4 Hz, H-4′), 7.67 (3H, m, H-3″, H-4″, H-5″), 7.42 (2H, t, $J_{2''(3'',5'')}$=$J_{6''(5'',3'')}$=9.3 Hz, H-2″, H-6″). EI-MS *m/z* (rel. int %): 256.2(67) (M^+), 135.2 (64), 1050(100), 77.0(70); HREI-MS: calculated for $C_{14}H_{12}N_2OS$; 256.0670, observed; *m/z* 256.0672.

2.2.2. 4-Fluoro-*N*-(phenylcarbamothioyl)benzamide (2):

White. Yield: 74%, m. p. 146-155°C. FT-IR (KBr pellet cm^{-1}): ν_{max} (N-H) 3272; (C-H) 2924; (C=S) 1257; (C=O) (C-F) 746. λ_{max}, nm (CH_3OH) (ϵ, $M^{-1}cm^{-1}$):209 (3966); 261 (5322); H^1-NMR (400 MHz, DMSO-d_6): δ 12.53 (1H, s, N-H), 11.59 (1H, s, N-H), 8.05 (2H, dd, $J_{3'',5''}$=5.6 Hz, H-3″, H-5″), 7.36 (2H, t, $J_{2''\ (3'',5'')}$ =$J_{6''(5'',3'')}$= 8.8 Hz, H-2″, H-6″), 7.26 (1H, t, $J_{4'(3',5')}$= 8.0 Hz, H-4′), 7.67 (2H, d, $J_{2'(3')}$=$J_{6'(5')}$= 7.7 Hz, H-2′, H-6′), 7.42 (2H, t, $J_{3'(2',4')}$=$J_{5''(4',6')}$= 7.6 Hz, H-3′, H-5′). EI-MS *m/z* (rel. int %): 274.2(49) (M^+), 135.0(70), 123.0(100), 95(62); HREI-MS: calculated for $C_{14}H_{11}FN_2OS$; 274.0576, observed; *m/z* 274.0564.

2.2.3. *N*-(2-Chloro(phenylcarbamothioyl)-4-fluorobenzamide (3):

White. Yield: 68%, m. p. 200- 210 °C. FT-IR (KBr pellet cm^{-1}): ν_{max} (N-H) 3307; (C-H) 3024; (C=S) 1234; (C=O) 1674; (C-Cl) 754;(C-F); 792; λ_{max}, nm (CH_3OH) (ϵ, M^{-1} cm^{-1}): 212 (6843); 261 (7900); ^{1}H-NMR (400 MHz, DMSO-d_6): δ 12.66 (1H, s, N-H), 11.83 (1H, s, N-H), 8.08 (2H, dd, $J_{3'',5''}$=5.3 Hz, H-3″, H-5″), 8.01 (1H, d, $J_{2'(3')}$= 7.6 Hz, H-2′), 7.58 (1H, dd, $J_{5'}$= 5.6 Hz, H-5′), 7.37 (4H, m, H-3′, H-4′, H-2″, H-6″). ESI-MS *m/z* (rel. int %): 309.0(62) (M^+), 311.0(24) (M^++2); HRESI-MS: calculated for $C_{14}H_{10}ClFN_2OS$; 308.7584, observed; *m/z* 309.7234.

2.2.4. *N*-(3,4-Dimethylphenylcarbamothioyl)-4-fluorobenzamide (4):

White. Yield: 88%, m. p. 157-166 °C. FT-IR (KBr pellet cm^{-1}): ν_{max} (N-H) 3350; (C-H) 2924; (C=O); 1666, (C=S); 1260, (C-F); 793; λ_{max}, nm (CH_3OH) (ϵ, $M^{-1}cm^{-1}$): 220 (8839); 265 (14678);^{1}H-NMR (400 MHz, DMSO-d_6): δ 12.43 (1H, s, N-H), 11.51 (1H, s, N-H), 8.02 (2H, dd, $J_{3'',5''}$= 5.4 H, €; 7900 L mol^{-1} cm^{-1}, H-3″, H-5″), 7.13 (1H , d, $J_{2'(3')}$= 7.6 Hz, H-2′), 7.37 (3H, m, H-3′, H-2″, H-6″), 2.19 (3H, s, CH_3), 2.18 (3H, s, CH3), 3.1 (1H, s, H-5′). EI-MS *m/z* (rel. int %): 302.2(19) (M^+), 163.1(31), 123.1(100), 95(40); HREI-MS: calculated for $C_{16}H_{15}FN_2OS$; 302.0889, observed; *m/z* 302.0886.

2.2.5. *N*-(4-Bromophenylcarbamothioyl)-4-fluorobenzamide (5):

White. Yield: 80%, m. p. 217-225 °C. FT-IR (KBr pellet cm^{-1}): ν_{max} (N-H) 3243; (C-H) 2927; (C=S) 1262; (C=O) 1667; (C-F) 758; λ_{max}, nm (CH_3OH) (ϵ, $M^{-1}cm^{-1}$): 215 (10056); 261 (15113); ^{1}H-NMR (400 MHz, DMSO-d_6): δ 12.46 (1H, s, N-H), 11.62 (1H, s, N-H), 7.63 (2H, d, $J_{3',5'}$= 9.3 Hz, H-3, H-5′), 7.57 (2H, d , $J_{2',4'}$ = 9.2 Hz, H-2′, H-4′), 8.02 (2H, dd, $J_{3'',2''}$=$J_{5'',6''}$= 5.6 Hz, H-3″, H-5″), 7.34 (2H, t, $J_{2''(3'',6'')}$=$J_{6''(5'',2'')}$= 8.8 Hz, H-2″, H-6″). EI-MS *m/z* (rel. int %): 352.0 (32) M^+,354.0(35) (M^++2), 213.0(64), 171.0(43), 123.0(100); HREI-MS: calculated for $C_{14}H_{10}N_2OSFBr$; 351.9681, observed; *m/z* 351.9692 (M^+).

2.2.6. 4-Fluoro-*N*-(4-methoxyphenylcarbamothioyl) benzamide (6):

White. Yield: 62%, m. p. 155-167 °C. FT-IR (KBr pellet cm^{-1}): ν_{max} (N-H) 3248; ν(C-H) 2926; (C=S) 1243; (C=O) 1665; (C-F) 781; λ_{max}, nm (CH_3OH) (ϵ, $M^{-1}cm^{-1}$): 211 (5628); 271 (6706);^{1}H-NMR (400 MHz, DMSO-d_6): δ 12.38 (1H, s, N-H), 11.53 (1H, s, N-H), 8.02 (2H, dd, $J_{3'',5''}$= 5.6 Hz, H-3″, H-5″), 7.54 (2H, d, $J_{3'(2')}$=$J_{5'(6')}$ = 8.8 Hz, H-3′,H-5′), 6.96 (2H, d, $J_{2'(3')}$=$J_{6'(5')}$ = 2.4 Hz, H-2′, H-6′), 7.36 (2H ,t , $J_{2''(3'',6'')}$=$J_{6''(2'',5'')}$ =8.8 Hz, H-2″, H-6″), 3.76 (3H, s, OCH_3). EI-MS *m/z* (rel. int %): 304.2(8) (M^+), 270.2(7), 165.7(18), 123.1(100), 95(25); HREI-MS: calculated for $C_{15}H_{13}FN_2O_2S$; 304.0682, observed; *m/z* 304.0672.

2.2.7 4-Fluoro-*N*-(2-methoxyphenylcarbamothioyl) benzamide (7):

White. Yield: 74%, m. p. 171-178 °C. FT-IR (KBr pellet cm^{-1}): ν_{max} (N-H) 3390; (C-H) 2930; (C=S) 1240; (C=O) 1677, (C-F); 747; λ_{max}, nm (CH_3OH) (ϵ, $M^{-1}cm^{-1}$) : 213 (6640); 321 (3760); ^{1}H-NMR (400 MHz, DMSO-d_6): δ 12.90 (1H, s, N-H), 11.79 (1H, s, N-H), 8.5 (1H,d, $J_{2'(3')}$= 9.3 Hz, H-2), 7.21 (1H , d , $J_{2'(3')}$ = 2.4 Hz, H-2′), 8.04 (2H, dd, $J_{3'',2''}$=$J_{5'',6''}$= 5.2 Hz, H-3″, H-5″), 6.99 (1H, t, $J_{5''(4'')}$=2.4 Hz, H-5″), 7.12 (1H, m, H-5″), 3.88 (3H, s, OCH_3). EI-MS *m/z* (rel. int %): 304.2(12) (M^+), 273.1(43), 165.1(14), 123.0(100), 95 (24); HREI-MS: calculated for $C_{15}H_{13}N_2O_2SF$; 304.0682, observed; *m/z* 304.0683.

2.3.8. *N*-(4-Chlorobenzothiazol-2-yl)-4-fluorobenzamide (8):

White. Yield: 52%, m. p. 291-300 °C. FT-IR (KBr pellet cm^{-1}): ν_{max} (N-H) 3230; (C-H) 2923; (C=S) 1232; (C=O) 1681; (C-F); 757; (C-Cl) 679; λ_{max}, nm (CH_3OH) (ϵ, $M^{-1}cm^{-1}$):222 (2840); 288 (1644); ^{1}H-NMR (400 MHz, DMSO-d_6): δ 13.03 (1H, s, N-H), 8.04 (2H, m, H-3′, H-5′), 8.20 (1H, dd, $J_{2''}$=5.6 Hz, H-2″), 7.92 (1H, m, H-5″), 7.27(1H, t, $J_{3'(2')}$ = 4.0 Hz, H-3′), 7.03 (1H, s, H-5′), 7.37 (1H, m, H-2′). EI-MS *m/z* (rel. int %): 306.2(40) (M^+), 307.2(18) (M^++2) 263.2(14), 140.1(20), 123.1(100), 95(77); HREI-MS: calculated for $C_{14}H_8ClFN_2OS$; 306.003, observed; *m/z* 306.0028.

2.2.9. 4-Fluoro-*N*-(2-methoxy-4-nitrophenylcarbamothioyl) benzamide (9):

Yellow. Yield: 81%, m. p. 202-210 °C. FT-IR (KBr pellet cm^{-1}): ν_{max} (N-H) 3242; (C-H) 2924; (C=S) 1251; (C=O) 1677; (C-O) 1027; (NO_2) 1327; λ_{max}, nm (CH_3OH) (ϵ, $M^{-1}cm^{-1}$): 211 (4769); 284 (6447); ^{1}H-NMR (400 MHz, DMSO-d_6): 13.34 (1H, s, N-H), 11.94 (1H, s, N-H), 8.06 (2H, t, $J_{3''(2'',4'')}$=$J_{5''(6'',4'')}$ = 7.0 Hz, H-3″, H-5″), 7.37 (2H ,t , $J_{2''(3'',6'')}$=$J_{6''(2'',5'')}$ =8.5 Hz, H-2″, H-6″), 9.10 (1H, dd, $J_{2'(3')}$=8.3 Hz, H-2′), 7.96 (1H, dd, $J_{3'(2',5')}$= 8.8 Hz, H-3′), 7.90 (1H, s, H-5′), 4.4 (3H, s, OCH_3). EI-MS *m/z* (rel. int %): 349.1(3) (M^+), 318.2(11), 210.0(9) 123.0(100), 95(50); HREI-MS: calculated for $C_{15}H_{12}N_3O_4SF$; 349.0533, observed; *m/z* 349.0534.

2.2.10. *N*-(2, 5-Difluorophenylcarbamothioyl)-4-fluorobenzamide (10):

White. Yield: 92%, m. p. 164-170 °C. FT-IR (KBr pellet cm^{-1}): ν_{max} (N-H) 3418.6; (C-H) 2925; (C=S) 1248; (C=O) 1676; (C-F) 711; λ_{max}, nm (CH_3OH) (ϵ, $M^{-1}cm^{-1}$): 212 (6310); 307 (4627);^{1}H-NMR (400 MHz, DMSO-d_6): δ 12.69 (1H, s, N-H), δ 11.90 (1H, s, N-H), 8.06 (2H, dd, $J_{3'',5''}$= 5.5 Hz, H-3″, H-5″), 8.13 (1H, m, H-5′), 7.36 (2H,t , $J_{2''(3'',6'')}$= $J_{6''(2'',5'')}$ = 8.9 Hz, H-2″, H-6″), 7.41(1H, m, H-4′), 7.2 (1H, m, H-3′) EI-MS *m/z* 310.2(52) (M^+), 291(16), 171.2(28), 123.1(100), 95(82); HREI-MS: calculated for $C_{14}H_9F_3N_2OS$; 310.0388, observed; *m/z* 310.0372.

2.2.11. *N*-(2,6-Diisopropylphenylcarbamothioyl)-4-fluorobenzamide (11):

White. Yield: 61%, m. p. 178-184 °C. FT-IR (KBr pellet cm^{-1}): ν_{max} (N-H) 3205; ν(C-H) 2964; ν(C=S) 1246; ν(C=O) 1674; ν(C-F); 7581. λ_{max}, nm (CH_3OH) (ϵ, $M^{-1}cm^{-1}$):215 (10201); 244 (12633);^{1}H-NMR (400 MHz, DMSO-d_6): δ 11.88 (1H, s, N-H), 11.62 (1H, s, N-H)), 8.05 (2H, dd, $J_{3'',2''}$=$J_{5'',6''}$= 5.4 Hz, H-3″, H-5″), 7.21 (2H,d, $J_{3',4'}$ =7.6 Hz, H-3′, H-5′), 8.62 (2H, t, $J_{2''(3'',6'')}$= $J_{6''(2'',5'')}$ =8.9 Hz, H-2″, H-6″), 7.30 (1H, t, $J_{3'(2',4')}$= 8.0 Hz, H-3′), 1.20 (6H, s, CH_3), 1.10 (6H, s, CH3). EI-MS *m/z* (rel. int %): 358.0(1) (M^+), 325.0(33), 315.0(69), 186.1(22), 122.9(100), 63(82); HREI-MS: calculated for $C_{20}H_{23}FN_2OS$; 358.4728, observed; *m/z* 358.4732.

2.2.12. 4-Fluoro-*N*-(4-(2-methoxyethyl)-2-methylphenylcarbamothioyl) benzamide (12):

Yellow orange. Yield: 55%, m. p. 154-160 °C. FT-IR (KBr pellet cm^{-1}): ν_{max} (N-H) 3350; ν(C-H) 2925; ν(C=S) 1235; ν(C=O) 1666; ν(C-O) 1090; ν(C-F) 735; λ_{max}, nm (CH_3OH) (ϵ, $M^{-1}cm^{-1}$): 213 (6617); 261 (6617);. ^{1}H-NMR (400 MHz, DMSO-d_6): δ 12.53 (1H, s, N-H), 11.58 (1H, s, N-H), 8.05 (2H, dd, $J_{3'',2''}$=$J_{5'',6''}$= 5.3 Hz, H-3″, H-5″), 7.65 (2H,d, $J_{2''(3'',6'')}$=$J_{6''(2'',5'')}$=9.0 Hz, H-2″, H-6″), 7.3 (2H, m, H-3′, H-5′), 7.3 (2H, d, $J_{2',3'}$= $J_{6',5'}$ = 9.0 Hz, H-2′, H-6′), 4.42 (2H, s, CH_2), 3.29 (1H, s, CH_3). EI-MS *m/z* (rel. int %): 318.2(9) (M^+), 259.2(13), 179.0(7), 122.9(100), 94.0 (35); HREI-MS: calculated for $C_{16}H_{15}FN_2O_2S$; 318.0838, observed; *m/z* 318.0854.

2.2.13. *N*-(3, 4-Dimethylphenylcarbamothioyl)-4-(trifluoromethyl) benzamide (13):

White. Yield: 88%, m. p. 254-260 °C. FT-IR (KBr pellet cm^{-1}): ν_{max} (N-H) 3277; ν(C-H) 2923; ν(C=S) 1259; ν(C=O) 1674; ν(C-F) 777; λ_{max}, nm (CH_3OH)(ϵ, $M^{-1}cm^{-1}$): 211 (6859); 268 (6161);^{1}H-NMR (400 MHz, DMSO-d_6): δ 12.56 (1H, s, N-H), 11.79 (1H, s, N-H), 7.40 (1H,s, H-5′), 8.13 (2H, d, $J_{3'',2''}$=$J_{5'',6''}$= 8.5 Hz, H-3″, H-5″), 7.90 (2H ,d , $J_{2''(3'',6'')}$= $J_{6''(2'',5'')}$=8.3 Hz, H-2″, H-

6″), 7.17 (1H, d, $J_{3'(2')}$=8.1 Hz, H-3′), 7.43 (1H, d, $J_{2'(3')}$= 8.64 Hz, H-2′), 2.21 (3H, s, CH_3), 2.22 (3H, s, CH_3). ^{13}C NMR (300 MHz, DMSO-d_6): δ 167.2 (C-1), 178.3 (C-2), 125.5 (C-7″), 136.6 (C-4″), 136.2 (C-1″), 132.5 (C-1′), 135.5 (C-4′), 134.5 (C-5′), 129.5 (C-5″, 3″), 125.3 (C-2″, C-6″), 121.5 (C-2′), 125. 1 (C-3′, 6′), 19.3 (C-7′), 18.9 (C-8′); EI-MS *m/z* (rel. int %):352.2(13) (M^+), 318.2(12), 173.0(100), 163.0 (27), 145.0 (59); HREI-MS: calculated for $C_{17}H_{15}N_2OSF_3$; 352.0857, observed; *m/z* 352.0876.

2.2.14. *N*-(4-(Trifluoromethoxy) phenylcarbamothioyl)-4-(trifluoromethyl) benzamide (14):

White. Yield: 79%, m. p. 169-178 °C. FT-IR (KBr pellet cm^{-1}): ν_{max} (N-H) 3227; ν(C-H) 2923; ν(C=S) 1275; ν(C=O) 1685; ν(C-O) 1012; ν (C-F) 717; λ_{max}, nm (CH_3OH) (ϵ, $M^{-1}cm^{-1}$): 208 (7918); 261 (9196);^{1}H-NMR (400 MHz, DMSO-d_6): δ 12.36 (1H, s, N-H), 11.89 (1H, s, N-H), 7.67 (1H,s, H-2′), 8.13 (2H, d, $J_{3'',2''}$=$J_{5'',6''}$= 8.2 Hz, H-3″, H-5″), 7.90 (2H ,d , $J_{2''(3'',6'')}$= $J_{6''(2'',5'')}$ = 7.6 Hz, H-2″, H-6″), 7.79 (2H, d, $J_{3',2'}$=$J_{5',6'}$= 9.0 Hz, H-3′, H-5′), 7.42 (2H, d, $J_{2',3'}$=$J_{6',5'}$= 8.4 Hz, H-2′, H-6′), 7.40 (1H, d, $J_{4'(5')}$= 8.4 Hz, H-4′).^{13}C-NMR (100 MHz, DMSO-d_6). EI-MS *m/z* (rel. int %): 408.2(17) (M^+), 349.2(10), 219.2(42), 173.0(100), 145.0(71); HREI-MS: calculated for $C_{16}H_{10}N_2O_2SF_6$; 408.3182, observed; *m/z* 408.0355.

2.2.15. *N*-(3-(Methylthio) phenylcarbamothioyl)-4-(trifluromethyl)benzamide (15):

Pale yellow. Yield: 94%, m. p. 138-146°C. FT-IR (KBr pellet cm^{-1}): ν_{max} (N-H) 3322; ν(C-H) 2921; ν(C=S) 1261; ν(C=O) 1671; ν(C-F) 796; λ_{max}, nm (CH_3OH) (ϵ, $M^{-1}cm^{-1}$): 215 (10503); 26 (10274);^{1}H-NMR (400 MHz, DMSO-d_6): δ 12.35 (1H, s, N-H), 11.83 (1H, s, N-H), 7.67 (1H,s, H-2′), 8.13 (2H, d, $J_{3'',2''}$=$J_{5'',6''}$= 8.0 Hz, H-3″, H-5″), 7.90 (2H ,d , $J_{2''(3'',6'')}$= $J_{6''(2'',5'')}$ = 8.3 Hz, H-2″, H-6″), 7.16 (1H, d, $J_{6'(5')}$= 7.4 Hz, H-6′), 7.35 (1H, t, $J_{5'(4',6')}$= 7.6 Hz, H5′), 7.40 (1H, d, $J_{4'(5')}$= 8.4 Hz, H-4′), 2.25 (3H, s, CH_3). EI-MS *m/z* (rel. int %): 370.2(23) (M^+), 336.2 (9), 173.1(100), 145.0(50); HREI-MS: calculated for $C_{16}H_{13}N_2OS_2F_3$; 370.0421, observed; *m/z* 370.0427.

3.0:Results and Discussion:

3.1.0. Chemistry:

Structure elucidation of a representative compound (**13**) is presented here. It was obtained as an amourphous white fluffy powderwith 88% yield.

High resolution mass, calculated for $C_{17}H_{15}N_2OSF_3$ (352.0857) was obtained by EI-MS technique, at*m/z* 352.0876 as the (M^+) molecular ion peak.The major fragments of the compounds appearded at 718.2, 173.0, and 146.2*m/z*. FT-IR spectra showed sharp and strong stretching frequencies for N-H, C-H, C=S, C=O and C-F at3277, 2923, 1259, 1674 and 777 cm^{-1}, respectively.

^{1}H-NMR spectroscopic study for compound **13** revealed that the protons of two secondary amines (a and b, Figure-1) appeared as singlet at δ 12.56, and δ 11.79, respectively.C-2″ and C- 6″ protons appeared at δ 8.13 as a doublet with *J*=8.3 Hz, because of same environment of aromatic ring. Similarly, two other aromatic protons of C-3″ and C-5″ resonated at δ 7.90 ppm (*J* = 8.5 Hz) as a doublet. One singlet of aromaticH-6′ appeared at δ 7.40. Proton C-2′ appeared at δ 7.43 (*J* = 8.6 Hz) as a doublet due to coupling with 3′ proton. WhileH-2′ resonated at the chemical shift δ 7.17as a doublet (*J* = 8.1 Hz).

^{13}C-NMR spectrum of compound **13** showed 16 carbon signals, including 7 quaternary carbons, 7 methine, and 2methyl carbons. Sulphur substituted quaternary carbon appeared as the most downfield carbon at δ 178.6. Carbon of C=O appeared at δ 167.2. Methine carbons of aromatic rings having similar environment appeared at δ 125.2 (C-3′/C-6′), δ 125.3 (C-2″/ C-6″), and 129.5 (C-3″/C-5″), whereas methine C-2′ appeared at δ 121.5. Two methyl carbons appeared at δ 135.5, and δ 134.5. Other quaternary carbons appeared at δ 136.2 (C-1″), 139 (C-4′), 136.5 (C-4″), and 134.5 (C-5′).

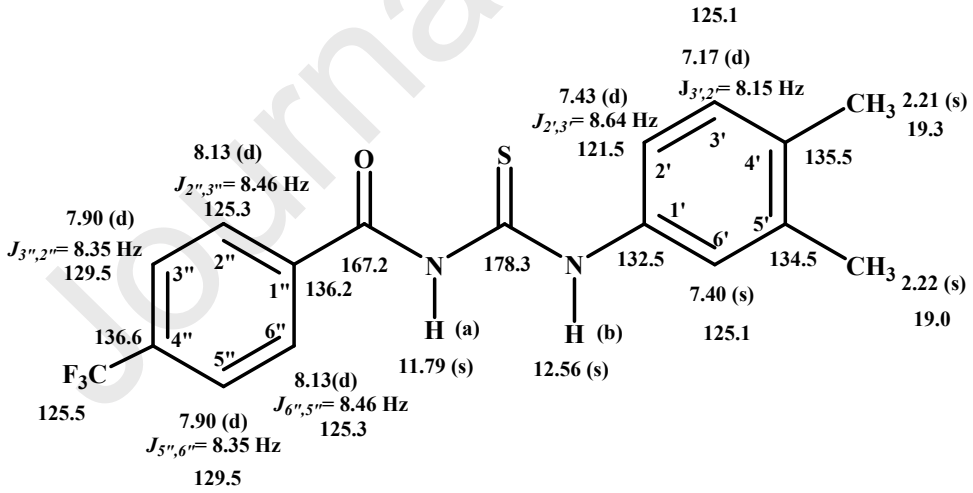

Figure-1: ^{1}H-NMR and ^{13}C-NMR peak assignment of compound **13.**

3.1.1. X-ray Diffraction Study:

3.1.1.1. Structure Features

The structure determination of compound **13** (Figure-2) represents that the structure is composed of a planar trifluoro methyl substituted benzoyl ring (C1-C6) and a dimethyl substituted phenyl rings (C9-C12) linked with each other *via* thiourea moiety along N1-C7 and N2-C9 bonds having length of 1.3588 Å, and 1.7521 Å. The dihedral angle between these planar rings was found to be 22.72^{o} with maximum deviation of 0.014(3) Å, for C9 from root mean square plane (r.m.s). The bond length for trifluoro methyl attached to C3 was found to be 1.4361(15) Å. The bond length for methyl substituent attached to C9 and C12 were found to be 15.081(3) Å, 15.042(3) Å, respectively.

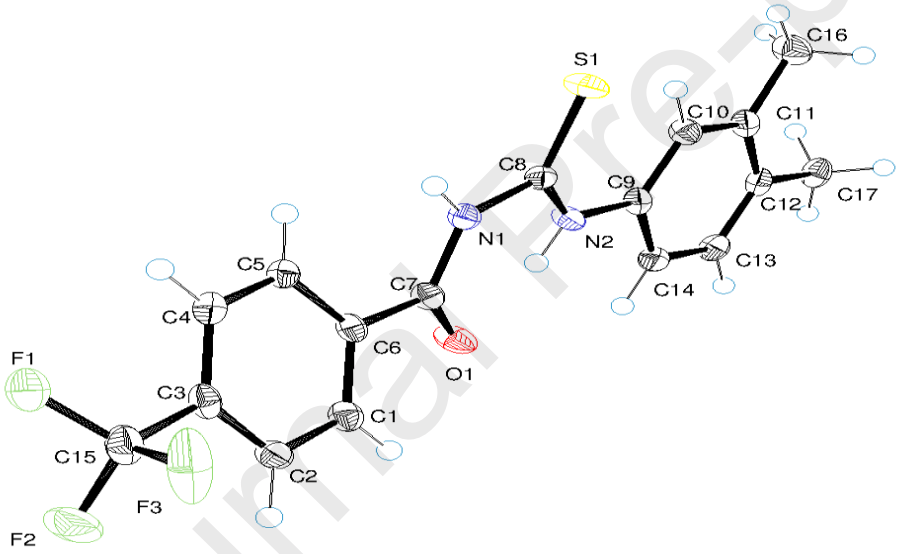

Figur-2: ORTEP view of X-ray structure of compound **13** at 50% ellipsoid probability.

3.1.1.2. Crystal Packing analysis

In the crystal lattice of compound **13** molecules were arranged in parallel repeating pattern running along c-axis (Figure 3) *via* N2—H2N---S1, C10—H10---S1, C11—H11---S1, and C17—H17A---F3, hydrogen bonds with donor to acceptor distances 3.5772 (2) Å, 3.213 (2) Å, 3.668 Å and 3.368 (3) Å, respectively. The geometry of this compound along thioamide linkage is stabilized

by intra-molecular hydrogen bonds N1—H1N_ _ _O1 and C5—H5_ _ _S1 to form S_6 graph set motif with donor to acceptor distance 2.645(3) Å and 3.195 (2) Å, respectively.

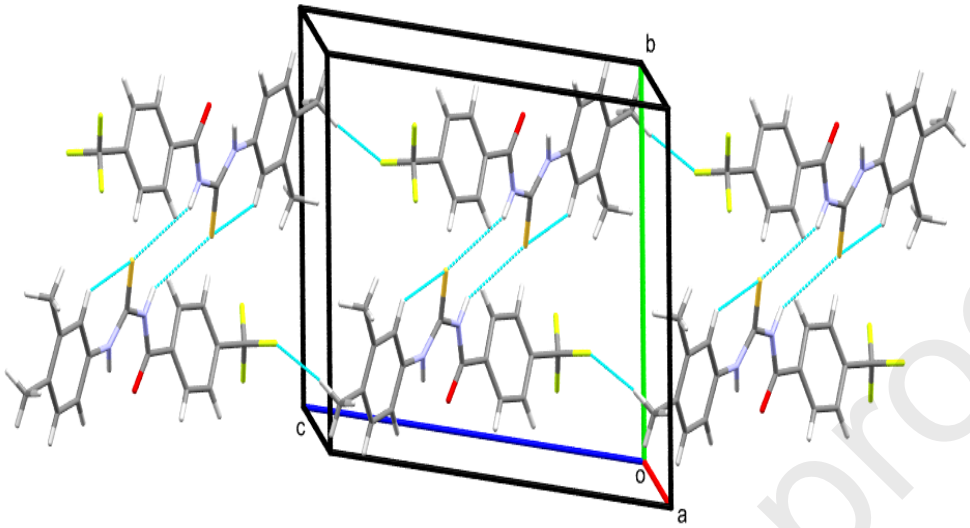

Figure-3: Arrangement and hydrogen bond interactions of molecules of compound **13** in crystal lattice.

3.1.1.3. Hirshfeld Surface

The Hirshfeld surface analysis is carried out (d_{norm}, curvedness and shape index) in order to analyze the intermolecular interaction within the crystal, and 2D fingerprint plots were generated by using Crystalexplorer3.1. The Hirshfeld surface analysis suggested that in compound **13** the major contributions towards the crystal packing include S---H (11.6%) and H---H (35.9%) followed by other interactions C-H (12.7%), F---H (11.7%), O---H (12.0%), and C---C (8. 7%).Two dimensional finger plots showing the occurrence of all intermolecular contacts is represented in Figure.4.

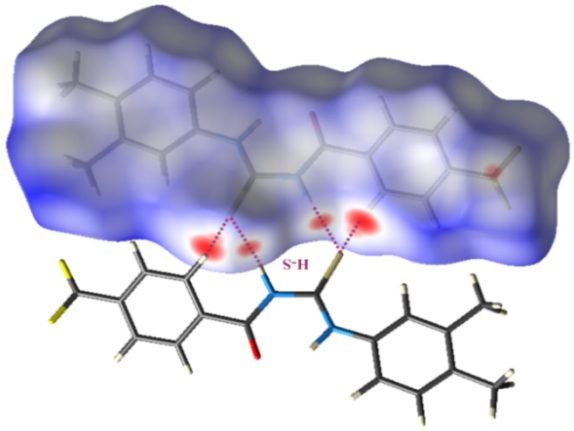

Figure 4: The d_{norm} mapped on Hirshfeld surface for visualizing the intermolecular contacts of the compound **13**.

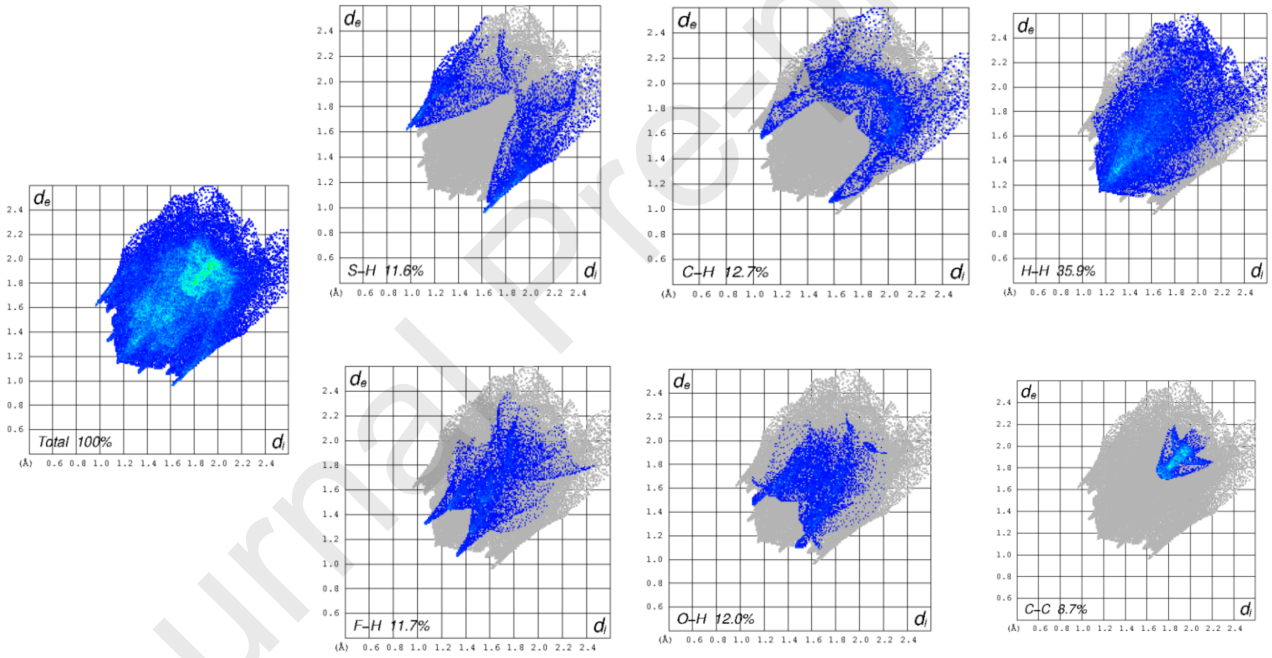

Figure 5: Two-dimensional fingerprint plot of compound **13** showing the percentage contribution of intermolecular interaction.

Table-1: Data Collection and refinement parameter of compound **13**

Empirical formula	$C_{17}\ H_{15}\ F_3\ N_2\ O\ S$
Formula weight	352.37
Temperature	100(2) K
Wavelength	1.54178 Å
Crystal system	Triclinic
Space group	P -1
Unit cell dimensions	a = 4.6790(4) Å α= 77.582(5) °
	b = 12.1130(11) Å β= 85.653(5)°
	c = 14.5622(14) Å γ = 89.977(5)°
Volume	803.60(13) $Å^3$
Z	2
Density (calculated)	1.456 Mg/m^3
Absorption coefficient	2.153 mm^{-1}
F(000)	364
Crystal size	0.280 x 0.070 x 0.040 mm^3
Theta range for data collection	3.117 to 68.181°.
Index ranges	-5<=h<=5, -14<=k<=14, -17<=l<=17
Reflections collected	21555
Independent reflections	2952 [R(int) = 0.0628]
Completeness to theta = 67.679°	99.8 %

Absorption correction	None
Refinement method	Full-matrix least-squares on F^2
Data / restraints / parameters	2952 / 0 / 219
Goodness-of-fit on F^2	0.829
Final R indices [I>2sigma(I)]	R1 = 0.0457, wR2 = 0.1159
R indices (all data)	R1 = 0.0544, wR2 = 0.1239
Extinction coefficient	n/a
Largest diff. peak and hole	0.500 and -0.298 e.$Å^{-3}$

3.2.0 Bioactivity Evaluation:

Compounds **1-15** were evaluated for their α-glucosidase inhibitory activity *in-vitro* by employing the reported procedure [25]. All tested compounds were found to be more active than the standard drug acarbose (IC_{50}=875.75±2.08 μM), except compounds **2**, **4**, **5**, **9,** and **14** which were found to be insoluble under required buffer conditions.

The parent compound **1** having unsubstituted benzene rings attached to thiourea moiety appeared as a potent inhibitor (IC_{50} = 171.21±0.23 μM) in comparison to the standard acarbose (IC_{50} = 875.75± 2.08 μM). In compounds **1** to **12** the R_1substituent is Fluorine atom which is substituted at *para* position of the phenyl ring, while the R_2 substituent was varied. Substitution of alkyl (-CH_3, -$CH(CH_3)_2$) alkoxy(-OCH_3), and halogens (Cl, Br, F) at different positions on benzamide ring showed variation in the α-glucosidase inhibitory activities. Compound **11** in which the R2 isdi-*ortho* isopropyl group was found to be the most active member of the series with IC_{50} = 40.9 ± 0.74 μM, followed by difluoro substituted phenyl ring in compound **10** (IC_{50}=34.63 ± 0.16 μM), further decrease in activity was observed in compound **3** (IC_{50} = 163.6± 0.61 μM) having chloro substituent at *ortho* position of the phenyl ring. Compound **7** with an *ortho*-alkoxy group showed more α-glucosidase inhibitory activity (IC_{50} = 105.2 ± 0.75 μM) than compound **6** having an

alkoxy substituent but at *para* position (IC_{50} = 333.41 ± 0.85 µM). A several fold decrease in the inhibitory activity observed in compound **12** in which the methoxy methyl group is present at *para* positions instead of alkoxygroup (IC_{50} =218.64 ± 1.14µM)

In compound **8** presence of heterocyclic ring with nitrogen and sulfur, fused with *ortho* chlorine substituted phenyl ring, showed a potent activity (IC_{50} = 20.44 ± 1.73 µM), made it the most potent compound in the series. SAR studies concluded that nitrogen and sulfur containing heterocyclic rings apparently contribute towards in significant inhibitory activity against α-glucosidase. Kinetic studies of compound **8** showed a non-competitive type of inhibition, it is revealed from inhibition pattern that compound **8** binds with allosteric site residues of the α-glucosidase.

In compounds **13-15**the R_1 (F) was replaced with trifluoromethyl group. Compound **13** having *para* and *meta*-methyl groups possessed potent inhibitory activity (IC_{50} = 60.41 ± 0.72 µM), which is further decreased in *para* trifluoro methoxy substituted compound **14** (IC_{50} = 92.36 ± 0.11 µM). In conclusion, SAR studies revealed that the number, position and nature of electron donating and withdrawing groups significantly alter the inhibitory potential of synthesized thiourea derivatives.

Compounds **1-15** were also evaluated for DPPH radical scavenging activity [26, 27]. and cytotoxicity against 3T3 mouse fibroblast cell line [28]. All compounds showed a weak to moderate activity against DPPH radical scavenging activity and non-cytotoxic in nature, except compound **12.**

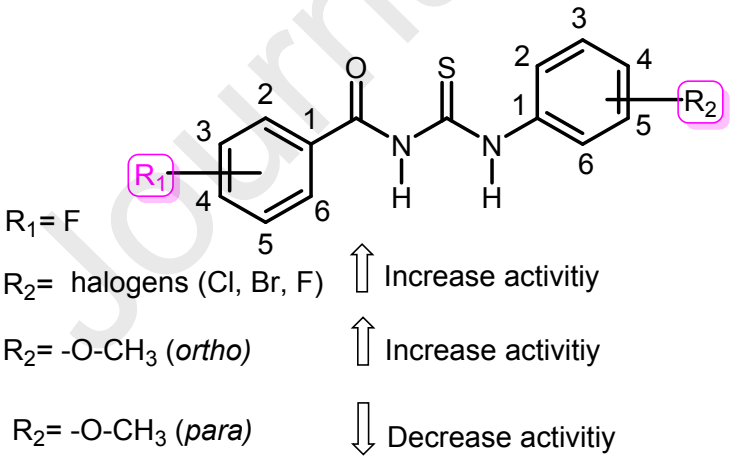

The summary of biological activity is given in Table 2.

Table 2: Summary of biological activities of compounds **1-15**

Comp.#	**-R_1**	**-R_2**	**α-G1ucosidase inhibition (anti-hyperglycemic) IC_{50}±SEM [μM]**	**DPPH Radical Scavenging Assay IC_{50}±SEM [μM]**	**Cytotoxicity Assay against 3T3 cell line IC_{50}±SEM [μM]**
1	-	-	171.21±0.23	NA	NA
2	4-Fluoro	-	ND	206.7±3.6	NA
3	4-Fluoro	2-Chloro	163.6±0.61	NA	NA
4	4-Fluoro	4,5-Dimethyl	ND	NA	NA
5	4-Fluoro	4-Bromo	ND	NA	NA
6	4-Fluoro	4-Methoxy	333.41 ±0.69	117.2±1.87	NA
7	4-Fluoro	2-Methoxy	105.2±0.82	209.3±2.12	NA
8	4-Fluoro	4-chloro-2-methylbenzo[d] thiazole	20.44±1.73	NA	NA

9	4-Fluoro	2-Methoxy, 4-Nitro,	ND	NA	29.1±1.9
10	4-Fluoro	2,5-Difluoro	34.63±0.16	NA	NA
11	4-Fluoro	2,6-Diisopropyl	40.9±0.74	NA	NA
12	4-Fluoro	4-Methoxymethyl	218.64±1.14	158.3±3.02	NA
13	4-Trifluoro	4,5-Dimethyl	60.41±0.72	226.5±0.34	NA
14	4-Trifluoro	4-Trifluoromethoxy	92.37±0.11	NA	NA
15	4-Trifluoro	3-Methylsulfane	ND	NA	NA
Standard	ACARBOSE		875.75±2.08	-	-
	GALLIC ACID		-	26±3.15	-
	CYCLOHEXAMIDE		-	-	0.8±0.20

*NA= Not active

*ND= Not dissolved

*SEM= Standard Error of Mean.

3.3.0 Kinetic Study:

Compounds **8** and **10** were selected for the evaluation of mechanism of inhibition. Lineweaver-Burk plots were used to determine the type of inhibition of α-glucosidase enzyme. The reciprocal of the rate of the reaction were plotted against the reciprocal of substrate concentrations to monitor the effect of the inhibitor on both $K_{m,}$ and V_{max} values.Compound **8** showed a non-competitive inhibition with K_i value 26.2 ± 0.018 µM, in this type of inhibition K_m remains constant and a decrease in V_{max} observed. Compound **10** appeared as a competitive inhibitor with the K_i 29.8 ± 0.0056 µM, with constant V_{max} and increasing K_m values.

Table 3: Kinetic study data of compounds **8**, and **9** as α-glucosidase inhibitors**.**

Compounds	**IC_{50} ± SEM**	**K_i ±SEM**	**Type of inhibition**
8	20.44±1.73	26.2 ± 0.018	Non-competitive
10	34.63±0.16	29.8 ± 0.0056	Competitive

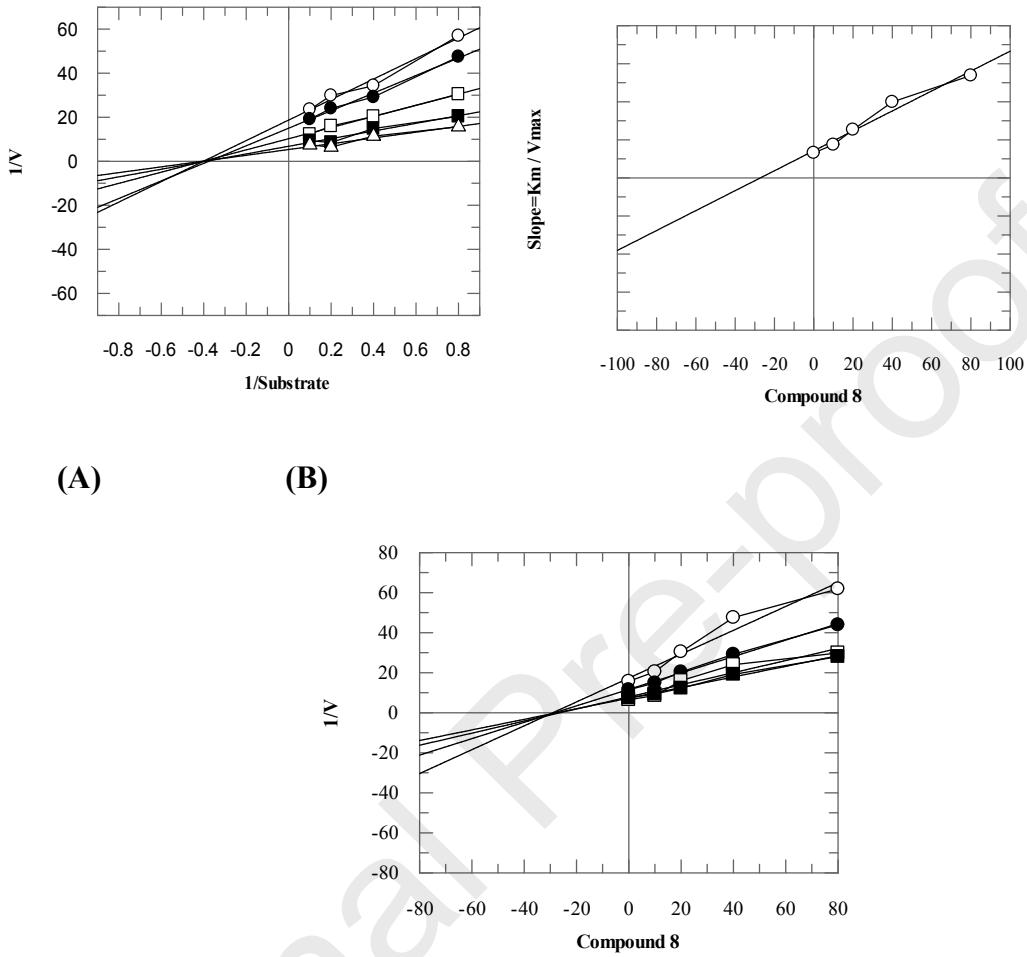

Figure 4: The inhibition of α-glucosidase by compound **8** (A) Linweaver-Burk plot of reciprocal of rate of reaction (velocities) *vs* reciprocal of substrate *p*-nitro phenyl-α-D-glucopyranoside in the absence of (-), and in the presence of 80µM (e), 40µM (f), 20µM (g) and 10µM (h) of compound **8**. (B) Secondary replot of Line weaver-Burk plot between the slopes of each line on Lineweaver-Burk plot vs different concentrations of compound **8**. (C) Dixon plot of reciprocal of rate of reaction (velocities) *vs* different concentrations of compound **8**.

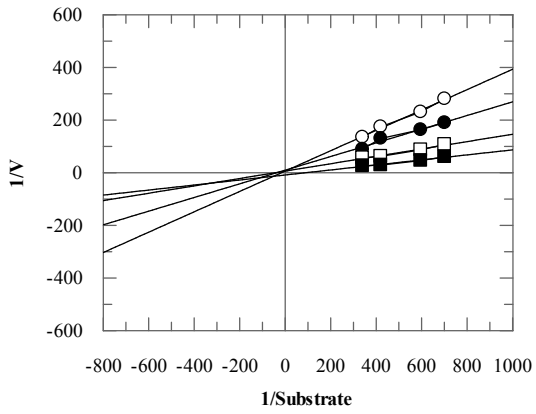

(A)

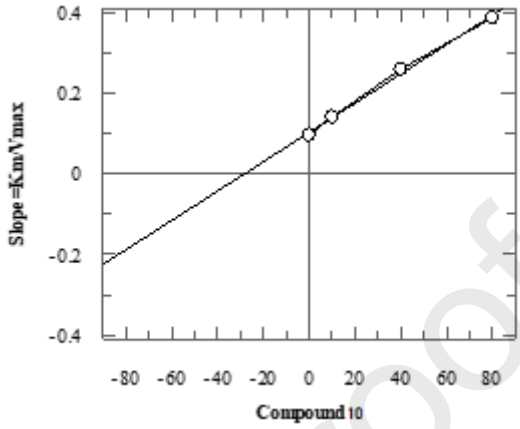

(B)

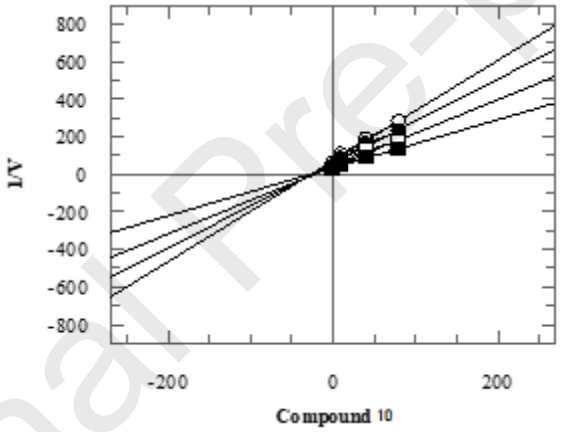

(C)

Figure 5: The inhibition of α-glucosidase by compound **10** (A) Lineweaver-Burk plot reciprocal of rate of reaction (velocities) *vs* reciprocal of substrate *p*-nitro phenyl-α-D-glucopyranoside in the absence of (-), and in the presence of 80µM (e), 40µM (f), and 10µM of compound **10**. (B) Secondary replot of Lineweaver-Burk plot between the slopes of each line on Lineweaver-Burk plot *vs* different concentrations of compound **10**. (C) Dixon plot of reciprocal of rate of reaction (velocities) *vs* different concentrations of compound **10**.

3.5.0. Statistical Analysis:

EZ-Fit Enzyme Kinetics Program (Perrella Scientific Inc. Amherst, USA) was employed to calculate the IC_{50} values. All the experiments were performed in triplicate, and variations in the results are reported in Standard Error of Mean values (SEM).

3.6.0. Conclusion:

In conclusion, we have synthesized a series of substituted benzamide based derivatives of thiourea as novel α-glucosidase inhibitors. The promising results of study concluded that these derivatives can be a potential candidate for further development and designing of new inhibitors of α-glucosidase enzyme, however further studies are required towards their development as anti-diabetic drug leads.

References:

[1] S. Kalra, Alpha glucosidase inhibitors, J. Pak. Med. Assoc. 64 (2014) 474–476 PMID: 24864650.

[2] C. Eleazu, A. Sampson, S. Saidu, K. Eleazu, C. Egedigwe-Ekeleme, Starch digestibility, polyphenol contents and in vitro alpha amylase inhibitory properties of two varieties of cocoyam (*Colocassia esculenta* and *Xanthosoma mafafa*) as affected by cooking, J. Food Meas. Charact. (2018) 1047–1053. https://doi.org/10.1007/s11694-018-9720-9.

[3] D. Halegoua-De Marzio, V.J. Navarro, Hepatotoxicity of cardiovascular and antidiabetic drugs, in: Drug-Induced Liver Dis. (Third Ed.), Elsevier, 2013: pp. 519–540 https://doi.org/10.1016/B978-0-12-387817-5.00029-7.

[4] S. Akhter, M. I. Choudhary, H. Siddiqui, S. Yousuf, Crystal structure and Hirshfeld surface analysis of *N*-(2-chlorophenylcarbamothioyl)-4-fluorobenzamide and *N*-(4-bromophenylcarbamothioyl)-4-fluorobenzamide, Acta Cryst. E: Crystallographic Communications 75(7) (2019) 1026-1029. https://doi.org/10.1107/S2056989019008569.

[5] Y. Zhang, X. Meng, H. Tang, M. Cheng, F. Yang, W. Xu, Design, synthesis, and biological evaluation of novel substituted thiourea derivatives as potential anticancer agents for NSCLC by blocking K-Ras protein-effectors interactions, J. Enzyme Inhib. Med. Chem. 35 (2020) 344–353.https://doi.org/10.1080/14756366.2019.1702653.

[6] D. Calla-Choque, F. Nava-Alonso, thiourea determination for the precious metals leaching process by iodate titration, Rev. Mex. Ing. Química. 19 (2020) 275–284. https://doi.org/10.24275/rmiq/IA539.

[7] V.S. Nagrare, B.B. Fand, V.C.B. Naik, B. Naikwadi, V. Deshmukh, D. Sinh, Resistance development in Cotton mealybug, *Phenacoccus solenopsis* Tinsley (Hemiptera: Pseudococcidae) to insecticides from Organophosphate, Thiadiazines and Thiourea derivatives, Int. J. Trop. Insect Sci. 40 (2020) 181–188. https://doi.org/10.1007/s42690-019-00068-9.

[8] A. Shakeel, A. A. Altaf, A.M. Qureshi, A. Badshah, Thiourea Derivatives in Drug Design and Medicinal Chemistry: A Short Review, J. Drug Des. Med. Chem. 2 (2016) 10–20. https://doi.org/10.11648/j.jddmc.20160201.12.

[9] D. M. Vardhan, H. K. Kumara, M. B. Sridhara, D. Gowda, Urea/thiourea derivatives of Gly/Pro conjugated 2, 3-dichlorophenyl piperazine as potent anti-inflammatory agents: SAR studies, Indian J. Chem. 56 (2017) 1207-1211. http://nopr.niscair.res.in/handle/123456789/43081.

[10] A. Maalik, H. Rahim, M. Saleem, N. Fatima, A. Rauf, A. Wadood, M.I. Malik, A. Ahmed, H. Rafique, M.N. Zafar, M. Riaz, L. Rasheed, A. Mumtaz, Synthesis, antimicrobial, antioxidant, cytotoxic, antiurease and molecular docking studies of *N*-(3-trifluoromethyl)benzoyl-N′-aryl thiourea derivatives, Bioorg. Chem 88 (2019) 102946. https://doi.org/10.1016/j.bioorg.2019.102946.

[11] S. Qaiser, M.S. Mubarak, S. Ashraf, M. Saleem, Z. Ul-Haq, M. Safdar, A. Rauf, T. Abu-Izneid, M.I. Qadri, A. Maalik, Benzilydene and thiourea derivatives as new classes of carbonic anhydrase inhibitors: an in vitro and molecular docking study, Med. Chem. Res. (2020). pp.1-12. https://doi.org/10.1007/s00044-020-02661-x.

[12] P. Cui, X. Li, M. Zhu, B. Wang, J. Liu, H. Chen, Design, synthesis and antibacterial activities of thiouracil derivatives containing acyl thiourea as SecA inhibitors, Bioorg. Med. Chem. Lett. 27 (2017) 2234–2237. https://doi.org/10.1016/j.bmcl.2016.11.060.

[13] S.S. Hassan, R.N. Shallan, M.M. Salama, Antibacterial and molecular study of thiourea derivative ligand and its Dimethyltin (IV) complex with the superior of its Copper (II) complex as a hepatocellular antitumor drug, J. Organomet. Chem. 911 (2020) 12115. https://doi.org/10.1016/j.jorganchem.2020.121115.

[14] C. Limban, A.V. Missir, M.T. Caproiu, A.M. Grumezescu, M.C. Chifiriuc, C. Bleotu, L. Marutescu, M.T. Papacocea, D.C. Nuta, Novel Hybrid Formulations Based on Thiourea Derivatives and Core@ Shell Fe3O4@ C18 Nanostructures for the Development of Antifungal Strategies, Nanomaterials. 8 (2018) 47. https://doi.org/10.3390/nano8010047.

[15] A.A. Spasov, A.N. Geisman, V.A. Kosolapov, D.A. Babkov, A.I. Rashchenko, V.A. Babkova, O.Y. Zakhar'yashcheva, A.A. Ozerov, Synthesis and Antiglycation Activity of Novel S-Carboxyalkyl Derivatives of 2-Thiouracil, Pharm. Chem. J. 53 (2019) 610–615. https://10.1007/s11094-019-02047-3.

[16] D.M.S. Vardhan, H.K. Kumara, H.P. Kumar, D.C. Gowda, Urea and Thiourea Derivatives of Dipeptides Conjugated Piperazine Analogue as A New Class of AGE's Inhibitors: Synthesis and Molecular Docking Studies, Asian J. Res. Chem. 10 (2017) 459–469. https://10.5958/0974-4150.2017.00075.

[17] M. Khan, N. Khan, K. Ghazal, S. Shoaib, Samiullah, I. Ali, M.K. Rauf, A. Badshah, M.N. Tahir, A.-U. Rehman, Synthesis, characterization, crystal structure, in-vitro cytotoxicity, antibacterial, and antifungal activities of nickel(II) and cobalt(III) complexes with acylthioureas, J. Coord. Chem. 73(12) (2020) 1790-1805. https://doi.org/10.1080/00958972.2020.1793136.

[18] N. Korkmaz, O.A. Obaidi, M. Senturk, D. Astley, D. Ekinci, C.T. Supuran, Synthesis and biological activity of novel thiourea derivatives as carbonic anhydrase inhibitors, J. Enzyme Inhib. Med. Chem. 30 (2015) 75–80. https://doi.org/10.1007/s00044-020-02661-x.

[19] G. Binzet, H. Arslan, U. Flörke, N. Külcü, N. Duran, Synthesis, characterization and antimicrobial activities of transition metal complexes of N, N-dialkyl-N′-(2-chlorobenzoyl) thiourea derivatives, J. Coord. Chem. 59 (2006) 1395–1406. https://doi.org/10.1080/00958970500512633.

[20] G. Binzet, N. Külcü, U. Flörke, H. Arslan, Synthesis and characterization of Cu (II) and Ni (II) complexes of some 4-bromo-N-(di (alkyl/aryl) carbamothioyl) benzamide derivatives, J. Coord. Chem. 62 (2009) 3454–3462. https://doi.org/10.1080/00958970903082200.

[21] B. Yu, Y. Liu, X. Peng, S. Hua, G. Zhou, K. Yan, Y. Liu, Synthesis, characterization, and antitumor properties of Au (i)–thiourea complexes, Metallomics. (2020) 104-113. https://doi.org/10.1039/C9MT00232D.

[22] W.I. Mortada, I.M.M. Kenawy, M.H. Abdel-Rhman, G.G. El-Gamal, S.M.N. Moalla, A new thiourea derivative [2-(3-ethylthioureido) benzoic acid] for cloud point extraction of some trace metals in water, biological and food samples, J. Trace Elem. Med. Biol. 44 (2017) 266–273. https://doi.org/10.1016/j.jtemb.2017.09.003.

[23] K.G. Akpomie, O.M. Fayomi, C.C. Ezeofor, R. Sha'Ato, W.E. Van Zyl, Insights into the use of metal complexes of thiourea derivatives as highly efficient adsorbents for ciprofloxacin from contaminated water, Trans. R. Soc. South Africa. 74 (2019) 180–188. https://doi.org/10.1080/0035919X.2019.1614695.

[24] G. Binzet, G. Kavak, N. Külcü, S. Özbey, U. Flörke, H. Arslan, Synthesis and characterization of novel thiourea derivatives and their nickel and copper complexes, J. Chem. 2013 (2013) 1-9. https://doi.org/10.1155/2013/536562.

[25] M.A. Bashir, K. Javaid, M. Shaikh, M.I. Choudhary, H. Siddiqui, Tyramine Derivatives as Potent Therapeutics for Type 2 Diabetes: Synthesis and In Vitro Inhibition of α-Glucosidase Enzyme, Med. Chem. (2020) 1124 - 1135. https://doi.org/10.2174/1573406416666200128114422.

[26] V.M. Thadhani, M.I. Choudhary, S. Ali, I. Omar, H. Siddique, V. Karunaratne, Antioxidant activity of some lichen metabolites, Nat. Prod. Res. 25 (2011) 1827–1837. https://doi.org/10.1080/14786419.2010.529546.

[27] J.M. Duarte-Almeida, A.V. Novoa, A.F. Linares, F.M. Lajolo, M.I. Genovese, Antioxidant activity of phenolics compounds from sugar cane (*Saccharum officinarum L.*) juice, Plant Foods Hum. Nutr. 61 (2006) 187. https://doi.org/10.1007/s11130-006-0032-6.

[28] M. Ayaz, M. Junaid, F. Ullah, A. Sadiq, F. Subhan, M.A. Khan, W. Ahmad, G. Ali, M. Imran, S. Ahmad, Molecularly characterized solvent extracts and saponins from Polygonum hydropiper L. show high anti-angiogenic, anti-tumor, brine shrimp, and fibroblast NIH/3T3 cell line cytotoxicity, Front. Pharmacol. 7 (2016) 74. https://doi.org/10.1002/slct.201901870.

GRAPHICAL ABSTRACT

Synthesis, Crystal Structure and Hirshfeld Analysis of Benzamide Derivatives of Thiourea as Potent Inhibitors of α-Glucosidase in-vitro

Sidra Akhter[a], Saeed Ullah[a], SammerYousuf[a], Atia-tul-Wahab[b], Hina Siddiqui, *[a] and M. Iqbal Choudhary*[a,b,c]

[a]H.E.J. Research Institute of Chemistry, International Center for Chemical and Biological Sciences, University of Karachi, Karachi-75270, Pakistan

[b]Dr. Panjwani Center for Molecular Medicine and Drug Research, International Center for Chemical and Biological Sciences, University of Karachi, Karachi-75270, Pakistan

[c]Department of Biochemistry, Faculty of Science, King Abdulaziz University, Jeddah-21452, Saudi Arabia

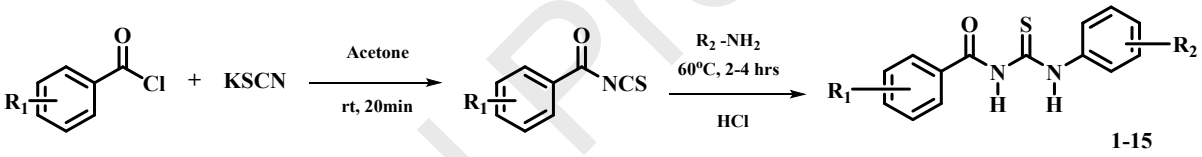

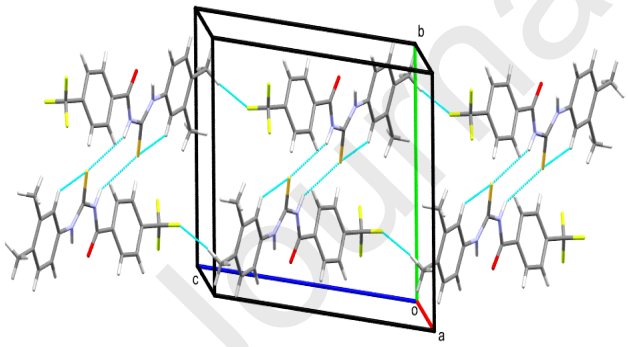

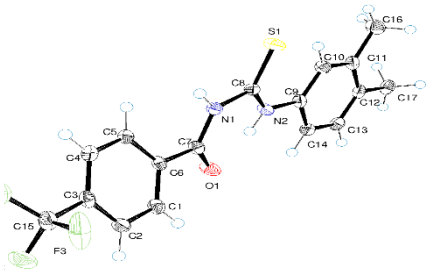

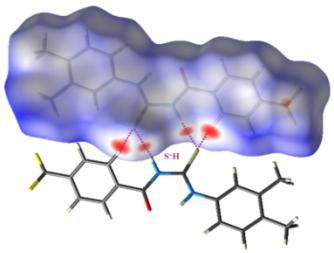

Synthesis, Crystal Structure and Hirshfeld Analysis of Benzamide Derivatives of Thiourea as Potent Inhibitors of α-Glucosidase in-vitro

Benzamide based structural analogues **1-15** were synthesized, and evaluated for α-glucosidase inhibition activity *invitro* for the first time. Compounds **1-9** were found to be known, while compounds **10-15** were found to be new. However, to the best of our knowledge we are reporting α-glucosidase inhibitory activity of these bezamide derivative of thiourea for the first time.

Compounds **1**, **3**, **6-8**, **10-14** were found to be potent α-glucosidase inhibitors within IC_{50} range of 20.44- 333.41 μM, in comparison to standard inhibitor, acarbose (IC_{50} = 875.75 ± 2.08 μM). Mode of the enzyme inhibition was determined on the basis of kinetic studies which demonstrated that compounds **8,** and **10** were non-competitive and competitive inhibitors of α-glucosidase enzyme, respectively.

Single crystal X-ray and Hirshfeld Surface analyses of a representative compound is also presented.

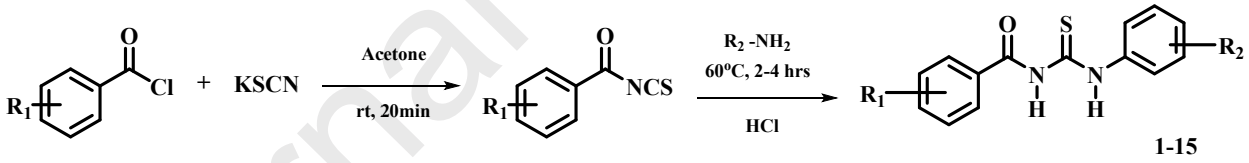

1-15

Declaration of interests

☒ The authors declare that they have no known competing financial interests or personal relationships that could have appeared to influence the work reported in this paper.

☐The authors declare the following financial interests/personal relationships which may be considered as potential competing interests: